Slow EIT waves as gravity modes

J. Vranjes
Belgian Institute for Space Aeronomy, Ringlaan 3, 1180 Brussels, Belgium

(Received 30 March 2011; accepted 15 May 2011; published online 15 June 2011)

The EIT waves [*named after the extreme-ultraviolet imaging telescope (EIT) onboard the solar and heliospheric observatory (SOHO)*] are in the literature usually described as fast magneto-acoustic (FMA) modes. However, observations show that a large percentage of these events propagate with very slow speeds that may be as low as 20 km/s. This is far below the FMA wave speed which cannot be below the sound speed, the latter being typically larger than 10^2 km/s in the corona. In the present study, it is shown that, to account for such low propagation speed, a different wave model should be used, based on the theory of gravity waves, both internal (IG) and surface (SG) ones. The gravity modes are physically completely different from the FMA mode, as they are essentially dispersive and in addition the IG wave is a transverse mode. Both the IG and the SG mode separately can provide proper propagation velocities in the whole low speed range. © *2011 American Institute of Physics*. [doi:10.1063/1.3597136]

I. INTRODUCTION

One of the most striking details related to so called extreme-ultraviolet imaging telescope (EIT) waves is the wide range of the propagation velocity reported in the literature. The velocities of 50–60 km/s were reported in Ref. 1, together with those of 350 km/s. In the same reference, values of 500 km/s are mentioned also as observed by Yohkoh/SXT (soft x-ray telescope). In Ref. 2, the values in the range 25–450 km/s are reported, observed by solar and heliospheric observatory (SOHO) EIT. Much more on that issue is available in Ref. 3, and also in Ref. 4 where velocities as low as 20 km/s are reported.

The EIT wave is usually described in terms of the fast magneto-acoustic (FMA) mode, which implies the phase propagation speed given by

$$v_p = \left(c_s^2 + c_a^2\right)^{1/2}, \quad c_s^2 = \frac{\kappa(T_e + T_i)}{m_i}, \quad c_a^2 = \frac{B_0^2}{\mu_0 m_i n_0}. \quad (1)$$

Clearly, the Alfvén velocity c_a, determined by two plasma parameters, gives some space to adjust to such a large span of values and even to provide the low values mentioned above. For example, taking $n_0 = 10^{16}$ m$^{-1/3}$, $B_0 = 10^{-4}$ T, and $n_0 = 3 \times 10^{14}$ m$^{-1/3}$, $B_0 = 2 \times 10^{-5}$ T, for c_a yields 22 km/s and 25 km/s, respectively. It remains questionable though how realistic such parameters are. Even the "classic" value of the phase speed of the EIT waves, that is around 250 km/s, implies $n_0 = 2 \times 10^{14}$ m$^{-1/3}$, $B_0 = 2 \times 10^{-4}$ T, hence, a rather low value for the magnetic field. The impression is that, to account for such speeds, certain values of the plasma-β are just adopted with the only purpose of fitting it into the assumed and pre-selected fast magneto-acoustic wave model. However, according to Ref. 3, out of 160 studied events of the EIT waves, more than 60% were with the speed below c_a.

On the other hand, the FMA wave speed includes the sound speed too. In calculating c_s, one has much less freedom for adjustment, because it is determined by the temperature only. For example, taking the ion and electron temperatures equal, and changing it in the range 0.6–2 million K, one obtains c_s in the range of 100–182 km/s. Thus, c_s remains above 10^2 km/s and no adjustment of the plasma-β may help. According to Eq. (1), there will always be $v_p \geq c_s$; therefore, the observed low values of v_p mentioned above (just a few tens of km/s) cannot possibly be explained within the fast magneto-acoustic wave model.

This inspired some researchers to make a completely different models, claiming that the EIT perturbations are not waves at all. Such non-wave models are merely focused on how the EIT perturbations are produced in the first place, e.g., due to some specific change in the magnetic field topology. However, the origin of perturbations is not an issue here. From basic plasma theory, we know that an initial perturbation, no matter how produced, will propagate as a wave, and regardless of its shape, it can be decomposed into Fourier harmonics. Hence, one has to deal with waves in any case.

What remains as one option is to search for some different wave model that could give proper propagation speed values in the low velocity range mentioned above. This should by no means reduce the validity of so widely accepted FMA wave model, which indeed seems to be able to capture many essential features of the fast EIT perturbations. Rather, it should represent a possible supplement in the slow speed domains where the FMA model appears to be not applicable. Regarding the waves propagating orthogonal to the magnetic field, that seems to be the case with the EIT perturbations, the choice is very limited, especially in view of the time and space scales involved in the perturbations. Yet, such plasma modes exist, and those are the internal gravity (IG) wave and the intermediate surface gravity (SG) wave, which have features completely different as compared to the FMA mode. Those features of interest for the EIT waves will briefly be described in the following sections.

II. INTERNAL GRAVITY WAVES

The physics of the IG wave is well known from standard books dealing with fluids in external gravity field, as excellent

examples to mention just the books of Kundu[5] and Sturrock[6], where the mode is described in the frame of ordinary single fluid theory. In the present two-component plasma case applicable to the coronal plasma, the starting equations for ions, in usual notation, are the continuity, momentum and energy equations, respectively,

$$\frac{\partial n_i}{\partial t} + \nabla \cdot (n_i \vec{v}_i) = 0, \tag{2}$$

$$m_i n_i \left(\frac{\partial}{\partial t} + \vec{v}_i \cdot \nabla \right) \vec{v}_i = -e n_i \nabla \phi - \nabla p_i + m_i n_i \vec{g}, \tag{3}$$

$$\left(\frac{\partial}{\partial t} + \vec{v}_i \cdot \nabla \right) \left(p_i n_i^{-\gamma} \right) = 0. \tag{4}$$

Here, the gravity is assumed in the z-direction, $\vec{g} = -g\vec{e}_z$, the ions are singly-charged, and ϕ is the electrostatic potential.

For low-frequency perturbations (with a phase speed much below the electron thermal velocity), electrons will be treated as isothermal, and their motion will be described by the quasi-neutrality condition $n_e = n_i$ (implying spatial scales far above the Debye length) and by the momentum equation in the inertia-less limit

$$0 = e n_e \nabla \phi - \kappa T_e \nabla n_e + m_e n_e \vec{g}. \tag{5}$$

The magnetic field is neglected and a proper justification for this will be given in the forthcoming text.

A. Equilibrium plasma

Assuming a static and isothermal equilibrium without electric fields, and for a constant gravity, for the density from Eqs. (3) and (5), one obtains the barometric formula

$$n_j \sim \exp(-z/H), \tag{6}$$

where $H = \kappa T_j/(m_j g)$ $(j = e,i)$ is the characteristic scale length for the stratified medium. Note that the same expression can be obtained for an ordinary neutral gas. According to the formula (6), there should be a difference (with height) in the density for species with different mass. In the case of electrons and ions, this would then violate the quasi-neutrality. To preserve the quasi-neutrality, the plasma will produce a macroscopic electric field $\vec{E}_0 = E_0 \vec{e}_z$ [known also as the Pannekoek-Rosseland (PR) field[7,8] or ambipolar gravity-induced field] which opposes the gravity in order to maintain its macroscopic quasi-neutrality. The electric field is oriented in such a way to lift the ions against the gravity and in the same time to pull the electrons down. Hence, the appropriate momentum equations for the two species will read

$$e n_0 E_0 + \kappa T_0 \frac{dn_0}{dz} + m_e n_0 g = 0, \quad E_0 = -\nabla \phi_0, \tag{7}$$

$$e n_0 E_0 - \kappa T_0 \frac{dn_0}{dz} - m_i n_0 g = 0. \tag{8}$$

Here, we used the quasi-neutrality $n_{i0} = n_{e0} = n_0$, and for simplicity the same temperature for both species is assumed. Subtracting the two equations yields the PR field

$$E_0 = \frac{(m_i - m_e)g}{2e} \simeq \frac{m_i g}{2e}. \tag{9}$$

Setting this into Eqs. (7) and (8), contrary to Eq. (6), one now finds *the same* distribution for both electrons and ions

$$n_0 = N_0 \exp\left(-\frac{z}{H_p} \right), \quad H_p = \frac{2\kappa T_0}{m_i g}. \tag{10}$$

It is seen that the plasma characteristic length H_p is twice larger than H for a neutral gas (obtained above also for ions without the effects of the PR field), and in the same time for electrons, it is shorter than H by a factor $2m_e/m_i$. These conclusions are general and valid for any external gravity field and plasmas with two species. Yet, these expressions are approximative because g and T_0 are assumed locally constant with height z. An application of this effect to ion acoustic (IA) oscillations can be found in Refs. 9 and 10. It can easily be shown that for two general species a and b, with the charge $-q_a$ and q_b, and with different temperatures $T_a \neq T_b$, the PR field will read

$$E_0 = g \frac{m_b T_a - m_a T_b}{q_a T_b + q_b T_a}. \tag{11}$$

Although frequently overlooked in the literature, this electric field is reality. The field of the same origin has been experimentally detected on the surface of metallic conductors.[11,12] It appears due to the redistribution of electrons and nuclei in metallic objects placed in the gravity field. In the case of an expanding atmosphere (e.g., in the solar wind), the magnitude of the electric field can substantially be greater than the Pannekoek-Rosseland value presented here. Details on that issue are available in Refs. 13 and 14.

The presence of *several charged ion species* may drastically change the previously obtained monotonous exponential distribution (10). To demonstrate this, one may assume the presence of l singly charged ion species of equal temperature and write the corresponding equilibrium momentum equations $-\kappa T \partial n_j/\partial z - n_j m_j g + e n_j E = 0$, $j = 1, \ldots l$. Performing a summation of the set of l equations, together with the electron equation, with the help of quasi-neutrality, $n_e = \sum_1^l n_j$, for the ambipolar electric field we obtain $E = \hat{m}(z) g/2e$. Here,

$$\hat{m}(z) = \sum_1^l m_j n_j(z) / \sum_1^l n_j(z), \tag{12}$$

is an effective, spatially dependent mean ion mass. Using these expressions in the equation for one specific j-th ion species, we obtain $d(\ln n_j)/dz = -[m_j - \hat{m}(z)/2]g/(\kappa T)$. It is seen that in fact it *yields a growth with* z as long as $m_j < \hat{m}(z)/2$. Hence, lighter ion species may have an inverse density distribution in lower layers. It may be concluded that in general $H_j = H_j(z)$, and this dependence includes a possible change of the sign too. Such distributions may be expected in environments with dominant heavy ions, details related to the terrestrial atmosphere are available in Ref. 15. In the corona, the situation is just the opposite; therefore, the effects of extra ion species will not be studied here. The

presented picture of the PR field and the change in the scale length (in the case of equal temperatures enlarging it by a factor 2 for protons and in the same time reducing it by a factor 1000 for electrons) are based on the model of a quiet, stratified fluid. However, turbulence and mixing of different layers, especially in the lower solar atmosphere, may effectively reduce its importance.

B. Small perturbations

Linearized momentum equations for the two species, with the help of Eqs. (7)–(10), become

$$m_i n_0 \frac{\partial \vec{v}_{i1}}{\partial t} = -e n_0 \nabla \phi_1 - \nabla p_{i1} - n_1 g m_i \frac{\tau}{1+\tau} \vec{e}_z, \tag{13}$$

$$0 = e n_0 \nabla \phi_1 - \kappa T_e \nabla n_1 - n_1 g m_i \frac{1}{1+\tau} \vec{e}_z. \quad \tau = \frac{T_i}{T_e}. \tag{14}$$

Note that the gravity term in the electron equation contains the ion mass. The gravity terms in the two equations are equal if $\tau = 1$, implying that the electrons and protons effectively behave as particles of the same weight (but with different inertia, hence 0 on the left-hand side in the electron equation). This is the consequence of the PR field. The other two linearized equations are

$$\frac{\partial n_1}{\partial t} + n_0 \nabla \cdot \vec{v}_{i1} + \vec{v}_{i1} \cdot \nabla n_0 = 0, \tag{15}$$

$$\frac{\partial p_1}{\partial t} - \frac{\gamma p_0}{n_0} \frac{\partial n_1}{\partial t} + n_0^{\gamma} (\vec{v}_{i1} \cdot \nabla)\left(p_0 n_0^{-\gamma}\right) = 0. \tag{16}$$

To satisfy flux conservation, the perturbations propagating in the (x,z)-plane are taken of the form[6,9,10]

$$n_1 = \hat{n}_1 \exp\left[-\frac{z}{2H} + i(k_x x + k_z z - \omega t)\right], \tag{17}$$

$$p_1 = \hat{p}_1 \exp\left[-\frac{z}{2H} + i(k_x x + k_z z - \omega t)\right], \tag{18}$$

$$v_{(x,z)1} = \hat{v}_{(x,z)1} \exp\left[\frac{z}{2H} + i(k_x x + k_z z - \omega t)\right], \tag{19}$$

$$\phi_1 = \hat{\phi}_1 \exp\left[\frac{z}{2H} + i(k_x x + k_z z - \omega t)\right], \tag{20}$$

where $\hat{\rho}_1$, etc., is used to denote the constant amplitude. Setting these expressions into Eqs. (13)–(16) yields the following equations for the amplitudes $\hat{n}_1, \hat{p}_1, \hat{v}_{x1}, \hat{v}_{z1}$:

$$\begin{gathered}
k_x \kappa T_e \hat{n}_1 + k_x \hat{p}_1 - \omega m_i N_0 \hat{v}_{x1} = 0, \\
\left[a m_i g + \left(ik_z + \frac{1}{2H_p}\right)\kappa T_e\right]\hat{n}_1 + \left(ik_z - \frac{1}{2H_p}\right)\hat{p}_1 \\
-i\omega m_i N_0 \hat{v}_{z1} = 0, \\
-i\omega \hat{n}_1 + ik_x N_0 \hat{v}_{x1} + \left(ik_z - \frac{1}{2H_p}\right) N_0 \hat{v}_{z1} = 0 \\
-i\omega\gamma \kappa T_i \hat{n}_1 - i\omega \hat{p}_1 + \frac{\kappa T_i N_0 (\gamma - 1)}{H_p} \hat{v}_{z1} = 0.
\end{gathered}$$

Here, $a = T_i/(T_e + T_i)$, the number of equations was reduced by eliminating the electrostatic potential by using the electron momentum equation. Its x-component gave $n_1/n_0 = e\phi_1/(\kappa T_e)$, while its z-component was identically equal to zero. Due to the shape of Eqs. (17)–(20), and after using Eq. (10), the common exponential term cancels out. After a few steps, this yields the dispersion equation

$$\omega^4 - \left[\omega_c^2 + v_s^2\left(k_x^2 + k_z^2\right)\right]\omega^2 + \omega_b^2 v_s^2 k_x^2 = 0. \tag{21}$$

Here,

$$\begin{aligned}
v_s^2 &= \frac{\kappa(T_e + \gamma T_i)}{m_i}, \quad \omega_c = \frac{v_s m_i g}{2\kappa(T_e + T_i)} = \frac{v_s}{2H_p}, \\
H_p &= \frac{\kappa(T_e + T_i)}{m_i g}, \quad \omega_b^2 = \frac{(\gamma - 1) m_i g^2 T_i}{\kappa(T_e + T_i)(T_e + \gamma T_i)}.
\end{aligned} \tag{22}$$

In H_p, the temperatures of the two species are kept different, ω_c is the IA wave cut-off frequency, and ω_b is the buoyancy [Brunt-Väisälä, BV] frequency.

Equation (21) describes the coupled IA and IG waves. The frequencies of the two modes are usually well separated, for comparison see a detailed analysis for ordinary fluids in Ref. 6. Hence, neglecting the last term in Eq. (21) yields the IA mode

$$\omega_{IA}^2 = \omega_c^2 + \left(k_x^2 + k_z^2\right) v_s^2. \tag{23}$$

On the other hand, in the low frequency range, one may neglect ω^4 in Eq. (21), which yields

$$\omega^2 = \frac{\omega_b^2 k_x^2 v_s^2}{\omega_c^2 + k^2 v_s^2} = \frac{\omega_b^2 k_x^2 v_s^2}{\omega_{IA}^2}, \quad k^2 = k_x^2 + k_z^2.$$

In case when $\omega_c^2 \ll k^2 v_s^2$, this yields the frequency for the IG mode presented in Ref. 5 for incompressible fluids and after using the Boussinesq approximation

$$\omega_{IG}^2 = \frac{\omega_b^2 k_x^2}{k_x^2 + k_z^2}. \tag{24}$$

According to conventional criterion of incompressibility, as long as the perturbed velocity $|v_1|$ is much below the sound velocity in the system, Eq. (24) will be valid. In fact, obtaining Eq. (24) was the main reason for the preceding text. Some well known and interesting properties of the IG mode can easily be seen by analyzing Eq. (24). The phase velocity of the mode is

$$\vec{v}_{IG} = \frac{\omega}{k^2}\vec{k} = \frac{\omega_b k_x}{k^3}(k_x \vec{e}_x + k_z \vec{e}_z). \tag{25}$$

On the other hand, its group velocity is

$$\vec{c}_{IG} = \vec{e}_x \frac{\partial \omega}{\partial k_x} + \vec{e}_z \frac{\partial \omega}{\partial k_z} = \frac{\omega_b k_z}{k^3}(k_z \vec{e}_x - k_x \vec{e}_z). \tag{26}$$

This yields

$$\vec{c}_{IG} \cdot \vec{v}_{IG} = 0. \tag{27}$$

From Eqs. (25)–(27), it is seen that the horizontal components of $\vec{c}_{IG}, \vec{v}_{IG}$ are in the same direction, while their vertical components are equal by magnitude and opposite. In general,

the vectors of the two velocities are perpendicular to each other, implying that the mode is hydrodynamically transverse, i.e., the fluid elements oscillate parallel to the lines of constant phase. From Eq. (25), it follows that the pure IG mode cannot propagate in the direction of the gravity vector (the phase velocity vanishes for $k_x = 0$), while its group velocity vanishes for $k_z = 0$ (no energy transfer by the IG wave for its purely horizontal propagation). For an oblique propagation, if the phase velocity has a positive z-component, the corresponding group velocity component is negative, and vice versa. In laboratory experiments with stratified liquids, e.g., a water with some vertical salinity profile [see Ref. 5 and references cited therein], any vertical or horizontal displacement due to some source will cause oblique IG waves, with vertical group velocity component dependent on the frequency. It turns out that the more frequent oscillation of the source, the more vertical transfer of the wave energy. An interesting application of these features to the heating of chromosphere by the IG waves has been proposed long ago.[16] Very recent observations in fact confirm that model,[17] showing that almost half of the required energy for the chromospheric heating comes from the IG waves launched from the photosphere.

However, its most important feature for the present study follows for a purely horizontal mode propagation. In such a case, the perturbations propagate in the direction in which the medium is isotropic, while their z-dependence is self-consistently taken into account through Eqs. (17)–(20); yet the two directions are not mixed, the corresponding characteristic scale-lengths are practically independent and the common exponential term then cancels out. In this limit from Eq. (24), it is seen that $\omega = \omega b_e$. Hence, the wave frequency achieves its maximum value, but more importantly, it becomes *independent on the wave number*. This further implies that, although the wave frequency is constant and strictly determined by the temperature and gravity [see Eq. (22)], the wave phase speed is $v_{ia} = \omega_b / k_x$. Being decoupled from the IA mode, the horizontally propagating IG waves are purely transverse, the actual displacement of the plasma due to the wave is in vertical direction, and, regardless of their wave-lengths, their frequency is constant. Hence, physically, the mode is completely different from the fast magneto-acoustic wave which, in the presence of a vertical background magnetic field $\vec{B}_0 = B_0 \vec{e}_z$, implies the density compressions in *horizontal* direction and the compressive component of the magnetic field in vertical z-direction.

Exactly because of such a geometry of the horizontally propagating IG mode, and, in particular, because of the *vertical displacement* of the plasma (i.e., along the magnetic field vector), the magnetic field was neglected from the beginning, because a plasma volume element moving up and down along the magnetic field lines due to the wave (propagating horizontally) will not be affected by the field. Of course, such an idealized picture will hold only as long as the frequencies of the two modes are well separated. Otherwise, there will be two physically rather different modes (the IG and the fast magneto-acoustic one), described by a dispersion equation similar to Eq. (21), but with the magnetic field effects included.

III. APPLICATION TO SLOW EIT WAVES

To get some feeling about the quantities defined above, adopting $T_e = T_i = 10^6$ K, $\gamma = 5/3$, and $g = 275$ m/s^2, one finds $v_s = 148$ km/s, $\omega_c = 1.23 \times 10^{-3}$ Hz, $\omega_b = 1.07 \times 10^{-3}$ Hz, and $H_p = 6 \times 10^7$ m. Note that the corresponding electron thermal velocity $v_{Te} = 4 \times 10^6$ m/s justifies the earlier used inertia-less electron limit.

Because ω_b is so close to ω_c, the two modes can only be well separated for large enough values of k_x. What "large enough" may mean is seen in Fig. 1, where the ratio of the internal gravity and ion acoustic wave phase velocities $v_{IG}/v_{IA} = \omega_{IG}/\omega_{IA} = \omega_b/(\omega_c^2 + k_x^2 v_s^2)^{1/2}$ is given in terms of the wave number k_x (multiplied by a factor 10^7) and for two plasma temperatures $T_e = T_i = T = 1 \times 10^6$ and 2×10^6 K. It is seen that the modes are well separated within a very large span of the wave-lengths that may be of interest for the EIT modes. However, for wavelengths of the order of 10^2 Mm (far left side in Fig. 1), the coupling with the acoustic mode should be taken into account.

For the value of $k_x = 4 \times 10^{-8}$ m^{-1} (i.e., $\lambda \simeq 150$ Mm), from the graph in Fig. 1, the phase speed v_{IG} becomes around 25 km/s. This perfectly describes the slow EIT perturbations. However, the constant frequency of the mode, $\omega_b = 1.07 \times 10^{-3}$ Hz, implies perturbations with the wave period $T = 2\pi/\omega_b$ of 98 min, that look too long. The wave period can become lower for shorter H_p. In fact, the value for H_p used above appears to be larger by a factor 2–3 from the values based on observations in coronal loops.[18] Hence, taking H_p shorter by a factor 3, the dispersion Equation (21) becomes modified. After solving such a new dispersion equation, we find $\omega_b = 0.0026$ Hz and, thus, the wave period $T = 2\pi/\omega_b = 40$ min. In addition, accounting for the presence of 10% of helium and calculating the mean density yields the mean ion mass equal to 1.3 proton mass, and with this the period can further be reduced to 35 min.

Clearly, the buoyancy frequency and the period of the IG wave are sensitive to small variations of parameters. The value for the wave period presented here is about the best that can be obtained from the present model. An additional improvement would be to include the magnetic field and to study the coupled FMA and IG modes. The actual displacements of the fluid due to these two modes (and this holds for the IA case above too) are in fact orthogonal to each other.

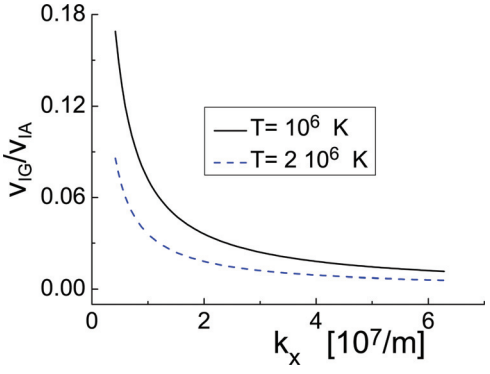

FIG. 1. (Color online) Ratio of the phase velocities (and frequencies) of the internal gravity mode and the ion acoustic mode, in terms of the wave-number.

So, the simple picture of the transverse (vertical) incompressible plasma displacement due to the IG mode alone will become much more complicated in the presence of the magnetic field and when the two modes are coupled. The coupling to the FMA mode will make the IG mode partly compressible too, and, in the same time, it will affect frequencies of both modes. This should particularly hold for a slightly oblique propagation with respect to the vertical direction, when the pure IG mode is described by Eq. (25). However, the magnetic field perturbations cannot be treated exactly within the present model. This is seen from the following. Having the magnetic field perturbed implies the use of the Ampère law

$$\nabla \times \vec{B}_1 = \mu_0 \vec{j}_1 = \mu_0 e n_0 (\vec{v}_{i1} - \vec{v}_{e1}). \tag{28}$$

In view of the earlier introduced variation of the velocity [Eq. (19)], and for the given equilibrium density variation [Eq. (10)], this would require that the variation of B_1 is the same as the variation of the density [Eq. (17)], $\sim \exp(-z/2H)$. However, one is supposed to use the Faraday law too, $\nabla \times \vec{E} = -\partial \vec{B}/\partial t$, where the variation of B_1 in the z-direction should be the same as the variation of the electric field potential [Eq. (20)], i.e., $\sim \exp(z/2H)$. Both are not possible, hence there can be no common exponential term to cancel out, and the given analytical model does not work. This case can only be studied numerically.

IV. SURFACE GRAVITY WAVE

The same procedure for obtaining the slow propagation velocity of the EIT waves within the IG wave scheme can be successfully extended to completely fill in the gap between the values obtained above (around 25 km/s in the given example), and the minimum possible velocity (i.e., c_s) that would follow from the fast magneto-acoustic wave model [which is $\geq 10^2$ km/s, see Eq. (1)]. Though this works only for the reduced H_p (by a factor 3) and for the mean ion mass equal to 1.3 proton mass, as explained in Sec. III. The maximum wave-lengths are below 200 Mm and wave periods are around 35 min.

However, even without such modifications, i.e., keeping the original H_p and m_i, the gap can be filled in also by using the SG waves in fluids with intermediate depths (comparable to the wave-lengths), by identifying the scale length H_p with the fluid depth. Performing derivations similar to Sec. II, the frequency of the gravity wave becomes[5]

$$\omega_{SG} = [g k_x \tanh(k_x H_p)]^{1/2}.$$

It should be stressed that a similar model is successfully used also in the description of terrestrial Rossby and gravity waves, where the bulk Earth's atmosphere is approximated by a layer of the thickness h obtained in the same manner as the quantities H and H_p earlier in the text.

The phase velocity $v_{SG} = \omega_{SG}/k_x$ of the surface gravity mode is given in Fig. 2 in the range of wave-lengths of interest for the EIT waves, for m_i equal to the proton mass, for the temperature of the plasma $T_e = T_i = 10^6$ K, and $H_p = 6 \times 10^7$ m as earlier. Here, the wave-length is taken in the interval 0.1–160 Mm, yielding the wave periods of the SG wave in the interval between 0.8 and 32 min, respectively. Hence, the surface gravity mode alone is capable of yielding proper propagation speeds for the EIT waves in the whole low velocity range. Regarding the coupling with the IA waves, similar arguments as in the previous text hold here too. However, because SG wave includes both vertical and horizontal plasma displacement, the coupling with the FMA wave is expected to be much more pronounced and it requires numerical simulations.

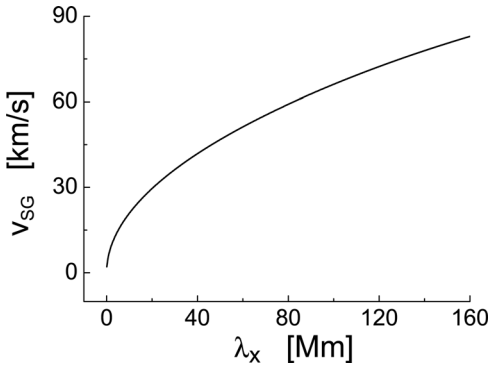

FIG. 2. The phase velocity $v_{SG} = \omega_{SG}/k_x$ of the surface gravity mode in terms of the wave-length.

V. CONCLUSIONS

The present study is focused on the slow range of the propagation speed of the EIT perturbations, i.e., those that are well below the magneto-acoustic velocity. Such low velocities, that do not fit into the fast magneto-acoustic wave description of the EIT perturbations, in the recent past have been a major argument against the wave nature of those events.

In this study, basic plasma and fluid theory are used in order to show that such slow propagating perturbations can successfully be described within the theory of gravity waves. In fact, two possible alternatives are suggested, based on the internal and surface gravity wave theory. Hence, these results should at least partly reestablish and support the wave-based model of the EIT perturbations.

In its simplest form, the internal gravity mode described in the text does not produce density variation. As already mentioned before, their coupling to the FMA mode in fact may include such variation. On the other hand, the horizontally propagating IG mode implies vertical displacements (in the z-direction) of the plasma, which means that layers of different density (with z) will be mixed together. For example, a denser plasma volume raised (within one half-length of the wave propagating in the x-direction) from some level z_0 to $z_1 = z_0 + \delta z_0$ will be surrounded by a less dense plasma corresponding to the level z_1 and vice versa in the other half-length. An observer will see a propagating perturbation accompanied by density variations, although the mode itself is not compressible in the first place.

The surface gravity mode is rather different, as it includes both horizontal and vertical displacements, and its group and phase velocities are in the same direction. Analysis of the fluid motion inside the wave[5,19,20] shows that in the wave crest, the fluid motion is generally in the direction of the wave, while in the troughs it is opposite. For a horizontal propagation, the group velocity is non-zero and the mode

transfers energy, which is not the case with the IG mode. This all should perhaps be a possible recipe for observations, to eventually distinguish the SG mode from both the IG and FMA modes. Though as a reaction to sudden perturbations (like flares), the coronal plasma can, at any time, support different plasma waves that on the other hand may become more or less coupled. Lack of ideal conditions, like for example the absence of a clear surface, implies that in a realistic situation some hybrid gravity mode may be expected that would include features of both gravity modes discussed in the text. The velocity and time and space scales of the resulting gravity mode should be between the two. A proper description of such waves and especially their coupling to FMA mode requires numerical simulations.

ACKNOWLEDGMENTS

This work has partly received funding from the Solar-Terrestrial Center of Excellence/SIDC, Royal Observatory of Belgium, Brussels.

[1]A. N. Zhukov and F. Auchère, Astron. Astrophys. **427**, 705 (2004).
[2]M. J. Wills-Davey, Astrophys. J. **645**, 757 (2006).
[3]M. J. Wills-Davey and G. D. R. Attrill, Space Sci. Rev. **149**, 325 (2009).
[4]A. N. Zhukov, L. Rodriguez, and J. de Patoul, Solar Phys. **259**, 73 (2009).
[5]P. K. Kundu, *Fluid Mechanics* (Acadamic, London, 1990).
[6]P. A. Sturrock, *Plasma Physics* (Cambridge University Press, Cambridge, 1994).
[7]A. Pannekoek, Bull. Astron. Inst. Neth. **1**, 107 (1922).
[8]S. Rosseland, Mon. Not. R. Astron. Soc. **84**, 720 (1924).
[9]C. Wahlberg and S. M. Revenchuk, Phys. Plasmas **10**, 1164 (2003).
[10]J. Vranjes, M. Y. Tanaka, and S. Poedts, Phys. Plasmas **11**, 4188 (2004).
[11]A. J. Dessler, F. C. Michel, H. E. Rorschach, and G. T. Trammell, Phys. Rev. **168**, 737 (1968).
[12]T. W. Darling, F. Rossi, G. I. Opat, and G. F. Moorhead, Rev. Mod. Phys. **64**, 237 (1992).
[13]J. Lemaire and M. Scherer, C. R. Acad. Sci. Paris **269B**, 666 (1969).
[14]K. Jockers, Astron. Astrophys. **6**, 219 (1970).
[15]J. Vranjes and M. Y. Tanaka, Phys. Scr. **71**, 325 (2005).
[16]B. W. Mihalas and J. Toomre, Astrophys. J. **249**, 349 (1981).
[17]T. Straus, B. Fleck, S. M. Jefferies, G. Cauzzi, S. W. McIntosh, K. Reardon, G. Severino, and M. Steffen, Astrophys. J. **681**, L125 (2008).
[18]I. De Moortel, C. E. Parnell, and A. W. Hood, Solar Phys. **215**, 69 (2003).
[19]N. Sepulveda, Phys. Fluids **30**, 1984 (1987).
[20]H. Ji, W. Fox, D. Pace, and H. L. Rappaport, Phys. Plasmas **12**, 012102 (2005).